Applied Geochemistry 112 (2020) 104474

Contents lists available at ScienceDirect

Applied Geochemistry

journal homepage: http://www.elsevier.com/locate/apgeochem

H_2 dynamics in the soil of a H_2-emitting zone (São Francisco Basin, Brazil): Microbial uptake quantification and reactive transport modelling

Andrey Myagkiy [a,b], Fabrice Brunet [a,*], Claudia Popov [c], Ricardo Krüger [c], Helena Guimarães [c], Rafaella Silveira Sousa [c], Laurent Charlet [a], Isabelle Moretti [b,d]

[a] Univ. Grenoble Alpes, Univ. Savoie Mont Blanc, CNRS, IRD, IFSTTAR, ISTerre, Grenoble, France
[b] Engie SA, Paris, France
[c] Enzymology Laboratory, Departamento de Biologia Celular, Universidade de Brasilia, Brasília, DF, Brazil
[d] E2S, University of Pau and the Pays de l'Adour, Pau, France

A B S T R A C T

Sandy kaolinite-rich soils, collected in a H_2-emitting circular depression (ca. 500 m in diameter), located in the São Francisco basin (Brazil), were exposed to H_2 gas concentrations in the 500–5000 ppm range for up to eight weeks. The samples were found to consume H_2 at a rate of approximately 0.05–0.1 mmol H_2/soil kg/day due to the microbial activity. DNA extraction from these soil samples before and after H_2 exposure, followed by Ribosomal Intergenic Spacer Analysis (RISA) and 16S rRNA gene amplicon sequencing, indicated that (i) the bacterial community is dominated by phyla that have been previously recognized to scavenge atmospheric H_2, and (ii) H_2 exposure leads to a significant modification of the bacterial community distribution. Measured H_2 uptake rates were fitted to the integrated form of the Michaelis-Menten equation and were further implemented in a 1-D reactive transport model. The model simulates gas-soil interactions in a 1-m vertical soil column, assuming homogeneous distribution of H_2-consuming bacteria. The evolution of the H_2 concentration in the unsaturated soil porosity along the column was simulated considering two different scenarios: a deep H_2 source (*Case 1*) and a biogenic surface source (*Case 2*). It was shown that, in the case of diffusion-dominated H_2-transport as considered in this study, bacterial activity will control the amplitude of the H_2 flux across the column. Moreover, we determined that bacterial activity can dramatically decrease the H_2 concentration in the soil porosity, by a factor of two compared to the source concentration. According to the simulation, the time-resolved concentration data collected in the São Francisco depression [*Prinzhofer* et al., *2019; International Journal of Hydrogen Energy*] are consistent with the combination of a deep (*Case 1*) and a surficial biogenic (*Case 2*) H_2 source in this locality.

1. Introduction

Dihydrogen (H_2) is an appealing source of energy that is expected to play a central role in energy transition. Currently however, H_2 is mostly produced by reforming of methane, a process which generates large amounts of CO_2. In the quest for "greener" hydrogen, natural sources of hydrogen are attracting increasing interest. Whereas different processes of natural H_2 production have been identified (*e.g.*, Wakita et al., 1980; Janecky and Seyfried, 1986; Savary and Pagel, 1997; Nandi and Sengupta, 1998), the evaluation of the H_2 resource volume and the definition of reliable exploration tools are two main scientific challenges that need to be tackled. To date, the only exploited geological accumulation of natural H_2 is located north of Bamako at Bourakebougou, in Mali. Since 2011, a pilot well has been producing a gas composed of 98% H_2 (Briere and Jerzykiewicz, 2016; Prinzhofer et al., 2018), which is converted into electricity for local use. Despite the known difficulty in storing H_2, a small and highly diffusive molecule, the Bourakebougou example demonstrates that natural H_2 can actually accumulate, at least transiently, in porous geological formations. Dolerite sills and aquifers have been identified as likely H_2-upward-migration barriers (Prinzhofer et al., 2018).

Whereas the background atmospheric H_2 concentration is close to 0.5 ppm (Ehhalt et al., 1977; Schmidt, 1978), H_2 concentrations above a few hundred ppm have been measured at approximately 1 m below the surface in circular depressions located in Central Russia (Larin et al., 2010, 2015), in the Carolina Bay, United States (Zgonnik et al., 2015), in Mali (Prinzhofer et al., 2018) and in South-Eastern Brazil (Prinzhofer et al., 2019). Dihydrogen daily emissions were estimated at a few thousandths to a few tenths of thousandths of cubic meters of H_2 per km^2. Prinzhofer et al. (2019) installed a series of seven H_2 sensors in a circular depression of the São Francisco basin (Minas Gerais, Brazil) in order to monitor H_2 soil concentrations at 80 cm depth. The soil H_2 concentration data have been collected since mid-2019, at 1-h intervals. The H_2 concentration dataset published in Prinzhofer et al. (2019) corresponds to the first 2 months of monitoring. Concentrations were found to be highly variable, with daily pulses lasting between 6 and 12

* Corresponding author.
E-mail address: fabrice.brunet@univ-grenoble-alpes.fr (F. Brunet).

https://doi.org/10.1016/j.apgeochem.2019.104474
Received 10 April 2019; Received in revised form 15 November 2019; Accepted 16 November 2019
Available online 18 November 2019
0883-2927/© 2019 Elsevier Ltd. All rights reserved.

h, and with a maximum of ca. 150 ppm occurring around noon. Prinzhofer et al. (2019) thus proposed that the corresponding H_2 pulses could result from an evaporation-type process, affecting the soil saturation degree and promoting deep-H_2 migration towards the surface. A single sensor (#9) recorded a contrasting signal of significantly higher concentration amplitude (ca. 1000 ppm) with a more complex variation pattern which likely indicates a different H_2 source-type. A deep origin for the São Francisco H_2 is suggested by the authors due to the presence of helium above atmospheric concentration in the gas sampled in the soil porosity (Prinzhofer et al., 2019). Nivin et al. (2016) monitored H_2-concentration in the cross-tunnel atmosphere of an underground mine (Kola Peninsula, Russia) over several years. They found similar H_2 concentration fluctuations (<300 ppm). The Fourier Transformation of the concentration signal revealed diurnal frequency patterns, among others, interpreted as the result of cyclic human operations in the mine.

In order to complement the first *in-situ* monitoring study of H_2 concentration in the porosity of soils by Prinzhofer et al. (2019), soil samples from the same instrumented circular depression were exposed to H_2 gas concentration pulses in the laboratory. In particular, the impact of H_2 exposure on the microbial community and activity was evaluated. A previous study by Sukhanova et al. (2013) on a similar ring-shaped depression located in a former arable field in western Russia (Lipetsk oblast), showed that H_2 release can lead to the degradation of humus, and that it also affects the microbial diversity. So far, soils have been considered as a major sink for atmospheric H_2, which is either consumed by bacterial metabolism or by abiontic soil hydrogenase (*e.g.*, Conrad and Seiler, 1981, 1985). As a consequence, the H_2 uptake by the uppermost soil compartment exposed to atmospheric gases, has been investigated in several field (*e.g.*, Conrad and Seiler, 1980; Yonemura et al., 1999), laboratory (*e.g.*, Trevors, 1985; Schuler and Conrad, 1990; Häring and Conrad, 1994; Gödde et al., 2000; Yonemura et al., 2000a, Smith-Downey et al., 2006) and numerical studies (*e.g.*, Yonemura et al., 2000b; Yashiro et al., 2011). However, H_2 is also an obligate by-product of biological N_2 fixation. In the rhizosphere of N_2-fixing nodules, H_2 can reach concentrations that largely exceed atmospheric concentration, a few centimeters away from the root nodules, (*e.g.*, La Favre and Focht, 1983). The response of soil microbiota to H_2 produced by N_2-fixing nodules has been studied experimentally by submitting soil samples to *ex-situ* H_2 at concentrations of hundreds to thousands of ppm (*e.g.*, Dong and Layzell, 2001; Khdhiri et al., 2015; Piché-Choquette et al., 2016), which are generally relevant to concentrations measured in the above mentioned circular depressions worldwide. The general view is that little, if any, of the nitrogenase-related H_2 production reaches the soil surface due to efficient consumption by H_2-oxidizing micro-organisms (Conrad and Seiler, 1979, 1980; La Favre and Focht, 1983; Popelier et al., 1985; Dong et al., 2003), implying strong local gradients of H_2 concentration.

In their experiments, Piché-Choquette et al. (2016) showed that soil exposure to H_2 had an impact on the microbial community and high-throughput sequencing revealed that bacterial communities were dominated by *Proteobacteria*, *Acidobacteria*, *Actinobacteria*, *Verrucomicrobia* and *Bacteroidetes*. Transcriptome analysis of *Chloroflexi*, which represents around 4% of total bacteria in soils (Delgado-Baquerizo et al., 2018), has shown that bacteria from this phyla oxidize hydrogen as an ecological strategy for survival in nutrient-scarce environments (Islam et al., 2019).

Soil uptake kinetics derived in the current study were incorporated in a 1-D diffusion reactive transport model in order to evaluate possible relationships between surface seeping and H_2 produced in the subsurface, and then conveyed towards the critical zone. The model provides insights into key parameters that may control hydrogen flux across soil horizons, and provides new constraints on H_2 dynamics in the São Francisco exhalation.

2. Materials and methods

2.1. Mineralogy and chemistry of the collected soil samples

Three soil samples were collected within (*BRAZIL 6* and *9*) or in the vicinity of (*BRAZIL 2*) the large circular structure (500 m across, Fig. 1) instrumented by Prinzhofer et al. (2019) and located in the São Francisco Basin (Brazil). *BRAZIL 6* and *9* were sampled at the exact location of sensors 6 and 9, respectively, deployed by Prinzhofer et al. (2019). Soil samples were collected at 15–40 cm depth and stored in the dark at ambient temperature (ca. 25 °C), in a closed bag. The soil color varied from greyish to brownish. Roots and larger soil aggregates were removed to select an optically homogeneous (particle and color) sample. In addition, a red acrisol from French Guiana, sampled at 70–80 cm depth, was selected (*GUIANA*), corresponding to sample II-2 in Guédron et al. (2009).

X-ray powder diffraction patterns of the Brazilian soil samples (*BRAZIL*) were found to match each other, with quartz and kaolinite as the main mineral constituents. Bulk chemical analyses (Table 1) confirmed a high SiO_2 content, over 75 wt%. Al_2O_3 content was between 5 and 8 wt%, which translates to a kaolinite content of 15–20 wt%. Minor Fe_2O_3 and TiO_2 components amounted to 0.4–0.6 wt% and 0.4–0.7 wt%, respectively. Iron was actually present as ferrous iron indicating reducing conditions. The organic carbon content of the *BRAZIL* soils comprised between 1.3 and 4.0%. Compared to the Brazilian samples, *GUIANA* is characterized by a much higher Al_2O_3 and Fe_3O_2 content, 22 and 36 wt%, respectively (Table 1), consistent with the presence of abundant goethite, hematite and gibbsite (Guedron et al., 2009). The carbon organic content (0.2%) of the *GUIANA* sample was the lowest among all studied samples. Note that *GUIANA* was stored for 15 years after collection.

2.2. H_2 – soil interaction set-up

One hundred and 50 g of soil, along with 20 ml of deionized water were loaded on a 300 ml stainless steel (Type 316) unstirred reactor (PARR®, USA). The reactor was sealed with a Teflon flat gasket, and fixed with six compression bolts to prevent gas leakages. The reactors were inserted into an aluminum block where the temperature was measured with a K-type thermocouple. Each reactor was equipped with both electronic and bourdon-tube pressure gauges. Once sealed, the reactor was flushed with argon prior to injection, at a pressure of up to 3 bars (Table 2) of an Ar/H_2 gas mixture with a H_2 concentration ranging between 2500 and 4000 ppmv. Gas – soil interaction was determined at

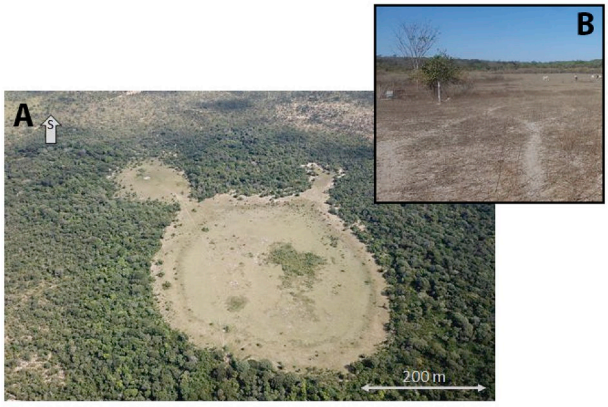


Fig. 1. Studied area where soil samples have been collected during the dry season (images taken in September 2018). (A) The circular depression, located in the São Francisco basin (Minas Gerais, Brazil), with a radius of ca. 500 m. (B) The sandy kaolinite rich soil is visible due to sparse vegetation in the center of the structure.

Table 1
Bulk analyses of the soil samples expressed in wt.% of oxides. *BRAZIL2a* was sampled just above *BRAZIL2* at a depth of 5–15 cm. *LOI*: lost on ignition (up to 1000 °C), *Corg*: organic carbon, *b.d.*: below detection limit. [1]Qualitative value of unknown uncertainty.

Sample	SiO_2	Al_2O_3	Fe_2O_3	FeO	MnO	MgO	CaO	Na_2O	K_2O	TiO_2	P_2O_5	*LOI*	*Corg*	Total
BRAZIL2	86.3	6.71	0.46	*0.17*	*b.d.*	0.04	0.05	*b.d.*	0.05	0.66	*b.d.*	4.9	0.23	99.19
BRAZIL2a	76.2	5.36	0.58	0.65	0.02	0.07	0.15	*b.d.*	0.07	0.41	*b.d.*	16.6	4.01	99.39
BRAZIL9	80.2	5.52	0.43	0.45[1]	b.d.	0.05	0.08	*b.d.*	0.06	0.54	*b.d.*	12.2	2.71	99.06
BRAZIL6	82.2	7.37	0.54	*0.54*	*b.d.*	0.04	0.05	*b.d.*	0.04	0.44	*b.d.*	8.3	1.39	98.97
GUIANA	19.2	21.92	36.24	1.23	0.03	0.12	*b.d.*	0.164	0.98	1.57	0.23	18.8	0.57	99.33

either room temperature (25 ± 3 °C) or 50 ± 3 °C. The gas from the headspace of the reactors was sampled on a time-resolved basis to monitor the H_2 concentration.

Prior to the experiments, each empty reactor was first tested for hydrogen leakage by loading an Ar/H_2 mixture (99.8/0.2 vol%) at 3 bars. After two weeks, H_2 concentration was found to differ by only 10 to 40 ppmv from the starting value, which is below the H_2 concentration measurement uncertainty threshold.

H_2 concentration in the gas was measured by means of a Clarus 500 gas chromatograph (GC) (PerkinElmer). The GC system has been optimized for H_2 gas analysis by using a 2 m long packed column, equipped with a molecular sieve (60–80 mesh, Supelco®), and a thermal conductivity detector (TCD). After being injected, the sample is vaporized and moves into the head of a chromatographic column where separation of gases occurs. Elution was brought about by the flow of inert carrier gas (Ar 5.0) at a pressure of 4 bars and flow rate of approximately 40 ml/min. The estimated uncertainty in gas measurement was approximately 5%.

The GC is calibrated with the use of a reference gas, injected in different proportional volumes to obtain a linear fitting curve (mV - ppm) for the dependency of the H_2 absolute concentration and the peak area.

2.3. DNA extraction-purification, ribosome intergenic spacer analysis (RISA) PCR and 16S rRNA gene amplicon sequencing

Total microbial community DNA present in the soil samples was extracted using the FastDNA® SPIN kit for soil (MP Biomedicals, Santa Ana, CA, USA). DNA was purified using the DNeasy Power Clean® Pro Cleanup kit (Qiagen, Venlo, Netherlands). Quantification of the purified DNA was performed using the Qubit™ dsDNA BR Assay kit (Invitrogen Waltham, MA, USA). All kits were used according to manufacturer's instructions. The integrity of the DNA was visualized by electrophoresis in a 1% agarose gel stained with ethidium bromide.

The intergenic spacer region (IGS) was amplified using 20 ng of purified DNA as a template in a 20 µl PCR reaction mixture containing: 1X PCR buffer, 1.5 mM $MgCl_2$, 2.5 mM dNTP mix, 2 U Platinum™ *Taq* DNA Polymerase (ThermoFisher Scientific, Waltham, MA, USA) and 10 pmol of each oligonucleotide primer. The bacterial IGS located between the small and large subunit rRNA genes were amplified with the following primers: S-D-Bact-1522-b-S-20 (5′-TGCGGCTGGATCCCCTCCTT-3′) and L-D-Bact-132-a-A-18 (5′-CCGGGTTTCCCCATTCGG-3′) (Normand et al., 1996). For fungi, primers were used to amplify the ITS1-5-8S-ITS2 region, representing consensus sequences found in various organisms at the 3′-end of the 18S rRNA genes (primer 2234C: 5′-GTTTCCGTAGGTGAACCTGC-3′) and at the 5′-end of the 26S rRNA genes (primer 3126T: 5′-ATATGCTTAAGTTCAGCGGGT-3′; Sequerra et al., 1997). The IGS for archaea (16S–23S) were amplified with primers 915f (5′- AAA GGA ATT GGC GGG GGA GCA C -3′) and 71r (5′- TCG GYG CCC GAG CCG AGC CAT CC-3′) (Garcia-Martinez and Rodriguez-Valera, 2000). PCR amplification for bacteria and archaea was performed using an initial denaturation step for 2 min at 95 °C, followed by 30 cycles of denaturation for 1 min at 95 °C, annealing for 1 min at 55 °C, and extension for 1 min at 72 °C, followed by a final extension for 5 min at 72 °C and cooling to 10 °C. The PCR amplification for fungi was performed with the same parameters described above, but with annealing temperature of 53 °C. PCR products were separated by electrophoresis for 2 h (for bacteria and fungi) and for 2 h 30 min (for archaea) at 45 V on a 6% polyacrylamide gel, stained with GelRed® Nucleic Acid gel Stain (Biotium, Fremont, CA, USA). Band profiles were analyzed with the software Bionumerics (Applied Maths, Sint-Martens-Latem, Belgium).

Amplicon DNA library preparation and sequencing were performed by Macrogen Inc. (Seoul, Korea) according to standard protocols. The metagenomic DNA samples from the soil were sequenced using the MiSeq Sequencing System (Illumina, San Diego, CA, USA). Paired-end sequencing was performed with a 2 × 300 bp run. Primers for the bacterial 16S rRNA gene were Bakt_341F: CCTACGGGNGGCWGCAG and Bakt_805R: GACTACHVGGGTATCTAATCC. Paired-end sequencing was performed with a 2 × 300 bp run. Raw paired-end Illumina sequences were preprocessed by removing Nextera adapters and Phix sequences with the bbduk program from the BBTools package (http://jgi.doe.gov/data-and-tools/bbtools/). Reads were then imported into QIIME2 (2018.4) as paired-ended and pair merging; quality control, 97% clustering, chimera removal along with taxonomy identification through the SILVA database (SILVA 132 99% OTUs full length sequences, 2018) where performed by plugins within the qiime pipeline available on the website.

2.4. 1-D modelling of H_2 diffusion-reaction in a soil column

A numerical model was developed using the numerical simulator COMSOL Multiphysics v 5.2 in order to simulate a 1-D diffusive transport of H_2 along a vertical 1-m long column. A biphasic partially saturated porous media was considered. The Michaelis-Menten kinetic law derived experimentally for H_2-consumption by microbial activity in the relevant soils, was incorporated into the numerical code. A homogeneous bacterial distribution and activity was assumed along the entire modeled column. The diffusive flux was modeled with the use of Fick's law, optimized for porous media, taking into account tortuosity, porosity and gas saturation. The gas molecular mean free path was assumed to be significantly larger than pore dimension. Therefore, no influence of pore walls was considered. Preferential transport pathways in the column soil due to the presence of cracks, worm channels or decayed and live root channels (*e.g.*, Nieber et al., 2013) were not considered in the model. Due to the poor solubility of H_2 gas in water at temperatures around 30–50 °C and close to ambient (Crozier et Yamamoto, 1974; Lopez-Lazaro et al., 2019), water was not regarded as a H_2 reservoir. Indeed, assuming a H_2 concentration of around 1000 ppm at the bottom of the column, which corresponds according to Dalton's law to 1 mbar of partial pressure, the solubility of H_2 in water at atmospheric pressure would result in 7.8×10^{-7} mol.L^{-1}, or 1.4×10^{-2} ppm. Together with the low diffusion coefficient of hydrogen in water (*e.g.*, Ferrell and Himmelblau, 1967), this transport mechanism appears to be negligible. H_2 adsorption by clay minerals was also ignored due to the poor H_2 sorption capacity reported by Truche et al. (2018) for kaolinite, which is the only clay mineral identified in the soils studied here. The effect of saturation was investigated at two different moisture levels, specifically high, 30%, and low, 10%, volumetric water contents. Larger values were not taken into account due to the overall dryness of the

Table 2
Dataset on Hydrogen experiments. C1, C2, C3, refer to the 1st, 2nd and 3[d] cycle, respectively; a, b, c, d refer to reactors 1, 2, 3 and 4, respectively.

Sample name	Initial [H_2] (mol.m^{-3}.kg^{-1})	Final [H_2] (mol.m^{-3}.kg^{-1})	Initial P (bar)	Final P (bar)	Fitted param. K_m; V_m; C	H_2 consumed (mol)	T (°C)	Cycle number	Cycle duration (days)
2.5 months after sampling									
Brazil 2_C1a	2.885	0.096	3.1	1.7	1.16; 0.51; 7.92	1.05E-04	25	1	13
Brazil 2_C1c	4.126	0.308	3.1	1.7	1.34; 0.58; 10.51	1.43E-04	25	1	13
Brazil 2_C2a	2.870	0.660	3.0	2.1	0.59; 0.23; 14.86	0.82E-04	25	2	14
Brazil 2_C2c	2.291	0.025	3.0	2.1	0.86; 0.45; 6.44	0.85E-04	25	2	14
Brazil2_C3a (autoclaving)	2.014	2.014	3.0	1.17	–	0	25	3	18
Brazil 2_C3c	2.009	0.147	3.0	1.17	32.86; 6.03; 4.01	0.75E-04	25	3	18
5 months after sampling									
Brazil 2_C1a	3.306	0.013	3.1	2.1	−1.24; 0.05; 36.43	1.24E-04	25	1	19
Brazil 2_C1c	3.656	0.012	3.1	1.7	−1.68; 0.05; 32.42	1.37E-04	25	1	13
2 weeks after sampling									
Brazil6_C1b	2.310	0.076	3.0	2.3	−0.01; 0.28; 8.22	0.84E-04	25	1	8
Brazil6_C1d	1.583	0.169	3.0	1.6	5.17; 7.56; 3.61	0.53E-04	25	1	18
Brazil6_C2b	3.127	0.025	3.0	2.3	0.34; 0.31; 10.44	1.16E-04	50	2	14
Brazil6_C3b	2.700	1.082	3.0	2.3	1.80; 0.27; 16.43	0.61E-04	50	3	12
6 weeks after sampling									
Brazil6_C1c	3.080	0.238	3.0	2.1	1.68; 0.70; 7.01	1.15E-04	50	1	12
Brazil6_C1d	3.851	0.180	3.0	2.1	6.89; 1.32; 9.58	1.37E-04	50	1	18
10 weeks after sampling									
Brazil6_C1a	2.275	0.252	3.0	2.1	1.94; 0.44; 9.15	0.75E-04	25	1	15
Brazil6_C1b	3.993	0.188	3.0	2.5	−0.16; 0.44; 9.01	1.43E-05	25	1	8
15 years after sampling									
Guiana #2b	1.890	0.001	3.0	2.3	–	0.71E-04	25	1	145
Guiana #4d	1.800	0.001	3.0	2.3	–	0.67E-05	25	1	145

region in July and August, *i.e.*, when the data published by Prinzhofer et al. (2019) were collected; the water table is located at approximately 3 m depth during this period. The diffusion coefficient was modified and corrected for the tortuosity factor, in order to obtain the effective diffusion coefficient for the hydrogen gas in a porous media. The modification was made as follows:

$$D^* = \Re * D_a \quad (1)$$

where, D^* is the effective diffusion coefficient for the hydrogen gas in a porous media, D_a is the diffusion coefficient of H_2 in air, and $\Re$ is defined as:

$$\Re = \varphi S_g \tau \quad (2)$$

where φ is the porosity, S_g is the gas saturation, and τ is the tortuosity, which is defined under the assumption of the widely used correlation of Millington and Quirk (1961):

$$\tau = \varphi^{1/3} S_g^{7/3} \quad (3)$$

Therefore, the final version of the transport equation that handles diffusive and advective H_2 migration in a gas phase of partially saturated porous media is:

$$\frac{\partial(\varphi S_g c_i)}{\partial t} + \nabla \cdot (u c_i) = \nabla \cdot (D^* \nabla c_i) + R^* \quad (4)$$

where, c_i is the concentration of H_2 in a gas phase within porous media, R^* is a rate of H_2 consumption by bacteria, and u signifies the gas velocity which is set to zero in our simulations apart from the sensitivity study, where the impact of advection is considered. We assumed changes in pressure gradient between pulsing deep source and surface to be low enough as to not be able to exceed the capillary forces, so that the water phase stays immobile.

Two idealized end-member cases were addressed in order to account for the H_2 concentration monitored in the São Francisco basin (Prinzhofer et al., 2019). The first case involved a deep H_2 source; the gas was assumed to vent upward into the overlying sediments and then undergo gas-soil interactions in the critical zone. In the second end-member case, it was assumed that H_2 was produced *in-situ* in the uppermost layer of the soil column. The latter modelling case was designed to evaluate whether H_2 produced at the surface could account for the H_2 concentrations measured at 0.8-m depth by Prinzhofer et al. (2019).

Under the assumption of a deeper source (Case 1), two general patterns of seepage were simulated and analyzed: i) gas seeps with constant H_2 concentration at the bottom of the modeled column, and ii) with a pulsating function of sinusoidal shape of variable period in order to produce changing H_2(g) emission concentrations over a day.

For the second case (Case 2), biogenic gas formation was considered with a positive correlation between H_2 production activity and soil temperature in order to reproduce the solar irradiance and H_2 concentration relationship evidenced by Prinzhofer et al. (2019). Producers were assumed to be homogeneously distributed with the consumers in the first 20 cm, while the other 80 cm of column were filled with H_2 consumers only. A biogenic H_2 production zone thickness of 20 cm was chosen because it bears temperature variations greater than 1–2 °C according to a heat equation. A process of evaporation has been considered in the upper soil zone and implemented as a fully gas-saturated region with fully evaporated water. The latter assumption is plausible since the water table is a few meters down (Prinzhofer et al., 2019), and the upper zone is not affected by the capillary fringe.

It should be noted that modelling was performed in the range of H_2 concentrations at which microbiological uptake kinetics was measured, *i.e.* in the 50–5000 ppm range. Modeled H_2 concentrations at the relevant soil column depth were expressed as a percentage of the source concentration. The H_2 concentration at the surface, or at the top cell of a modeled column, were set to zero in all simulated cases.

3. Results and discussion

3.1. H_2 uptake by soil samples

A total of eighteen H_2-exposure experiments were performed on four different soil samples at 25 and 50 °C (Table 2). Apart from the case where the soil sample was previously autoclaved at 120 °C in the reaction vessel, H_2 concentration in the headspace gas (termed $[H_{2,g}]$ hereafter) was found to decrease with time (Table 2), indicating an overall H_2 uptake by all samples. Such behavior is consistent with H_2 consumption associated with soil microbiological activity as already evidenced in previous laboratory studies (Table 3). Selected responses to H_2 exposure in the soil samples studied here are displayed in Fig. 2. Samples were submitted to up to three H_2-exposure cycles (Table 2); H_2-rich gas was re-injected into the autoclave once the H_2 concentration of the previous cycle had reached a concentration below ca. 100 ppmv.

Two and a half months after collection in the field, the *BRAZIL2* sample began to consume H_2 readily after 24 h (Fig. 2). With initial H_2 concentrations in the headspace of 2000–5000 ppmv, *BRAZIL2* was found to consume H_2 at a rate of up to 0.08 mmol $kg^{-1}d^{-1}$, corresponding to a $[H_{2,g}]$ decrease of around 300–400 ppmv per day in the reactor headspace (Fig. 2a). Such a consumption trend was maintained from the onset of the experiment, and throughout its course until the $[H_{2,g}]$ level in the autoclaves reached ~1000 ppm. For $[H_{2,g}]$ below ~ 1000 ppm, the H_2 up-take slowed, leading to a noticeable curvature on the corresponding $[H_{2,g}] = f(t)$ curve (Fig. 2a). The dependency of $\frac{\partial[H2,g]}{\partial t}$ on a residual concentration is consistent with previous studies (*e.g.*, Häring and Conrad, 1994; Dong and Layzell, 2001; Piché-Choquette et al., 2016) which inferred that H_2-consumption follows a Michaelis-Menten kinetics behavior. We thus fitted our H_2 uptake data to the integrated form of the Michaelis-Menten equation (Eq. (5) below):

$$v = -dC/dt = V_M C(t) / (K_M + C(t)) \quad (5)$$

where v is the overall velocity of the reaction, V_M is the maximum velocity, K_M is the Michaelis-Menten constant, C is the H_2 gas concentration, and t is time.

The integrated form of Equation (5) may be written as Equation (6):

$$t = \frac{-(K_M * ln\, C(t) + C(t))}{V_M} + A \quad (6)$$

The kinetic parameters, V_M (mol.m^{-3}.kg^{-1}.d^{-1}) and K_M (mol.m^{-3}.kg^{-1} as C(t)) as well as the A constant were retrieved using the least-square regression method (Fig. 3), and are given in Table 2. The

Table 3
Bacterial up-take rates from the literature and this study.

Up-take rate mmol.$kg^{-1}d^{-1}$	Sample characteristics	Reference
~120 (LA-HOB) [a] ~2 (HA-HOB) [a]	Upper 10 cm (combisol/luvisol)	Häring&Conrad (1994)
~30 (LA-HOB) [a] ~0.00004 (HA-HOB) [a]	Farmland soil	Piché-Choquette et al. (2018)
~7 [a]	3 weeks H_2 pre-treated, exposed $[H_2]$ < 2000 ppm, LA-HOB.	Dong and Layzell (2001)
~0.00005 [a]	Air treated control, exposed $[H_2]$ < 350 ppm, HA-HOB	
0.03–0.08	Reduced kaolinite sand (30–45 cm) exposed to $[H_2]$ < 3500 ppm; Km = 9300 ppm, Vm = 5.31 nmol $g^{-1}.h^{-1}$,	This study
0.2–0.6	Monoculture plots and grassland, exposed 525 ppm H_2	Khdhiri et al. (2015)

[a] Calculated for a H_2 concentration of 2000 ppm and a soil density of 2 g/cm^3.
LA-HOB and HA-HOB: Low- and High-affinity H_2-oxidizing bacteria, respectively.

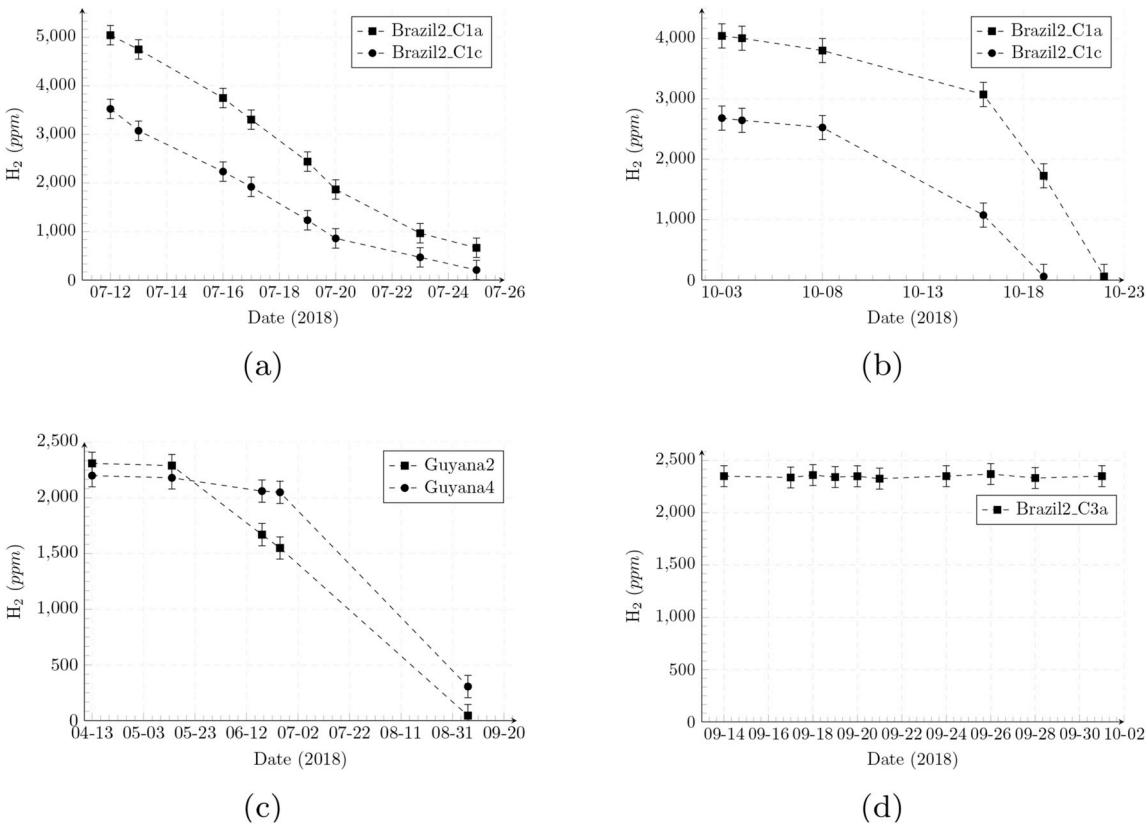


Fig. 2. Hydrogen consumption tests in (a) *BRAZIL2* sample (2.5 months after collection in the field), (b) *BRAZIL2* sample (5 months after collection), (c) *GUIANA* samples from outside the field of hydrogen emission (15 years after collection), (d) Sterilized *BRAZIL2* soil sample after autoclaving at 120 °C.

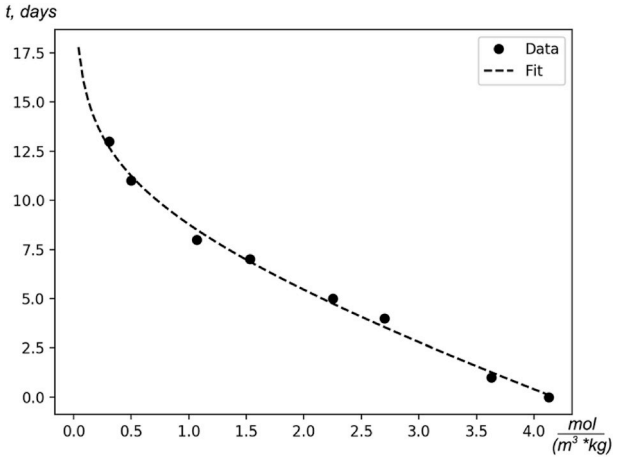


Fig. 3. Time – concentration curve of hydrogen consumption fitted by Michaelis-Menten kinetics equation. Representative sample: *Brazil2_C1c*.

BRAZIL2 soil sample, which was analyzed less than three months after its collection in the field, showed very similar consumption behavior (*BRAZIL2_C1a*, *BRAZIL2_C1c*, and *BRAZIL2_C2c*), and the corresponding kinetics parameters were taken as the basis for further numerical simulations.

Whereas H_2 uptake by the *BRAZIL2* sample, 2.5 months after collection, occurs readily after the beginning of the H_2 exposure, a significant latency time was found when the sample was stored for a longer time (5 months). Indeed, after 5 months storage, a bowed consumption curve was measured that initially had upward concave shape, eventually turning to be of downward concave shape (Fig. 2b). The latter suggests that the reactivity and consumption potential of microbial communities in *BRAZIL2* soil had dramatically decreased. The beginning of the consumption curve was characterized by a weak hydrogen consumption rate, as low as 40 ppm per day. Nevertheless, a subsequent gradual increase of the consumption rate was observed with time upon contact of hydrogen gas with the soil microbial community (Fig. 2b). After 13 days the consumption rate in both autoclaves reached values of 300–400 ppm, as was the case for *BRAZIL2* experiments analyzed 2.5 months after sample collection.

The effect appears to be even more pronounced in the *GUIANA* acrisol which was (1) stored for 15 years and (2) presumably never exposed to hydrogen concentrations above atmospheric. Here, we observed a latency time of several weeks before H_2 consumption was triggered (Fig. 2c). During this period H_2 up-take does not occur, or occurs at a relatively low rate (~10 ppm a day), implying very limited hydrogen-consuming microbiological activity.

The exposure of *BRAZIL6* samples to H_2 at 50 °C (Table 2) led to a H_2 uptake rate two times lower than the rate obtained at 25 °C. This is in agreement with Trevors (1985) and Smith-Downey et al. (2006) who inferred an optimum H_2-consumption temperature in the 20–30 °C range.

In order to verify the assumption of H_2-uptake resulting from microbiological activity in the soil, a reactor containing *BRAZIL2*, and which showed H_2-consumption in two successive cycles, was held for 20 min at a temperature of 120 °C. After this *in-situ* sterilization procedure the reactor was cooled down to ambient temperature and H_2 was injected again. The experiment (*BRAZIL2_C3a*, Table 2) was stopped after 18 days without any noticeable changes in H_2 concentration.

Finally, the H_2 consumption rates that were obtained here for *BRAZIL2* and which have been further implemented in our reactive transport model, are 5–10 times lower than those derived by Khdhiri et al. (2015), and reported in Table 3. However, Khdhiri et al. (2015)

showed that uptake rate is proportional to the carbon content of the soil which, in our case (0.23 wt%, Table 1), was 5–10 times lower than in their samples. The rates obtained here fall in the lower range of published data on H_2 uptake by soils and can be as much as three to four orders of magnitude lower than some studies on low-affinity H_2-oxidizing bacteria (*e.g.*, Häring and Conrad, 1994, Table 3).

3.2. Microbial community and impact of H_2 treatment

Total DNA extracted from soil samples was used to amplify the IGS with RISA-specific primers for bacteria, archaea and fungi (Fig. 4). DNA extraction was performed on *BRAZIL2* before and after H_2 exposure (*BRAZIL2_C3a* and *BRAZIL2_C3c*, respectively). For simplification, these latter three samples are termed 1.0, 1.1 and 1.2 (Table 2). Similarly, *BRAZIL9* and *BRAZIL9_C3b* are termed 3.0 and 3.1 (Table 2), respectively; *BRAZIL6* is 2.0; and *GUIANA*, *GUIANA4* and *GUIANA2* are 4.0, 4.1 and 4.2, respectively.

It can be readily seen on the dendograms that 2.0 and 3.0, which were collected on the same day, close to sensors 6 & 9 respectively, are very similar in their bacterial and archaeal content, which can be observed in the similarity and intensity of the dominant bands (Fig. 4). Interestingly, these two sensors yielded very different H_2 signals.

Sample 1.0, which was sampled at a different time of year (3 months earlier), in the same emitting structure, shows significant differences compared to the 2.0 and 3.0 samples. The sequenced 16S rRNA gene amplicon indicates that starting soils 1.0 and 3.0 are indeed different and dominated by *Chloroflexi* (28% and 18%, respectively), *Actinobacteria* (18% and 25%), *Proteobacteria* (18% and 16%), *Acidobacteria* (14% and 10%) and *Firmicutes* (4% and 16%), which represent 83% and 85% of the whole bacterial/archaeal content, respectively (Fig. 5). The thick bands of the fingerprint for archaea represent three major phyla: *Thaumarchaeota*, *Euryarchaeota* and *Crenarchaeota*. Fungal ITS amplicons were not sequenced (Fig. 4).

Dendogram analysis shows that samples 1.0 and 1.2 host distinct microbial communities (Fig. 4); as sample 1.2 is basically sample 1.0 that has been exposed to H_2 at 25 °C, changes in microbial community can thus be related to H_2 treatment. Major changes involve *Acidobacteria* increase from 14 to 22% and *Actinobacteria* decrease from 18% to 8% (Fig. 5). Both samples share 214 sequences from a total of 363 obtained for bacterial and archaeal diversity (Fig. 6b). These changes might be limited due to the fact that the samples already arise from a H_2-rich natural environment. For a more complete study of the possible impact of hydrogen treatment on soil microbiota, we analyzed, in addition to bacteria, the archaeal and fungal profile of the samples. The composition of bacteria and archaea appears to change with hydrogen treatment (Piché-Choquette et al., 2016; Perner et al., 2010). However, to our knowledge, neither archaea nor fungi have yet been described as H_2 consumers. Variations in the band positions and brightness were also observed in archaeal and fungal profiles between 1.0 and 1.2 (Fig. 4), and so the trend observed for bacteria seems also to hold for archaea and fungi.

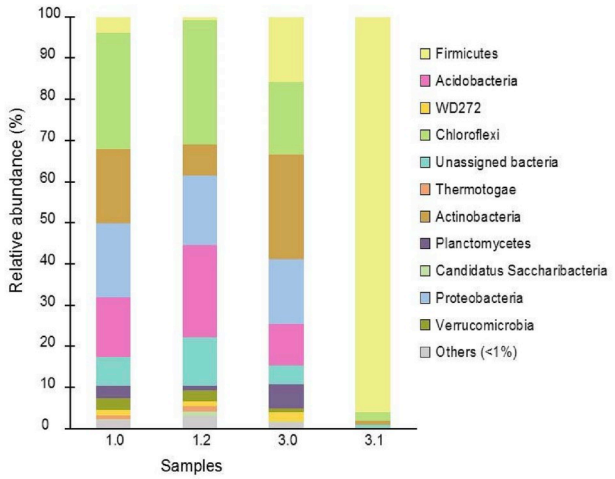


Fig. 5. Summary of Operational Taxonomic Units (OTU) showing different relative frequency abundance between treated (3.1 and 1.2) and non-treated H_2 soils (3.0 and 1.0).

Sample 1.1, which was autoclaved after H_2 treatment, is characterized by the absence of DNA. Sample 3.1 could not be amplified with archaeal and fungal RISA primers, and shows a single band on the bacterial profile (not shown). When compared to the starting soil sample 3.0, it appears that both abundance and composition of the bacterial communities were strongly affected by the H_2 treatment at 50 °C, which resulted in a drop in phyla diversity with the *Firmicutes* taxonomic group

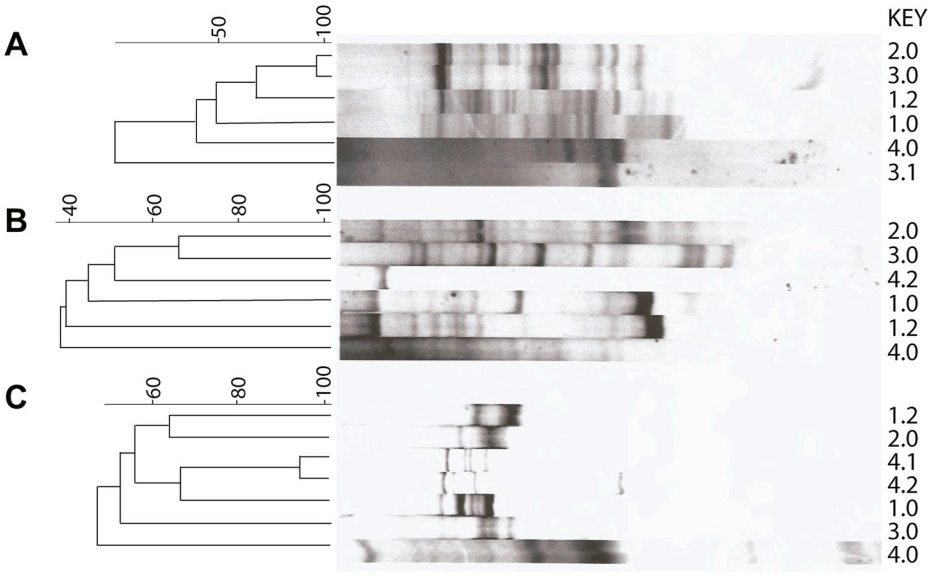


Fig. 4. RISA fingerprinting profiles of DNA extracted from the soil with dendograms showing similarities among soil communities for *A*: bacteria, *B*: archaea, and *C*: fungi. Each lane represents a different sample obtained with PCR amplification of the intergenic spacer region (IGS) with specific primers. Different bands represent distinct communities within each sample. Dendograms performed with Bionumerics software.

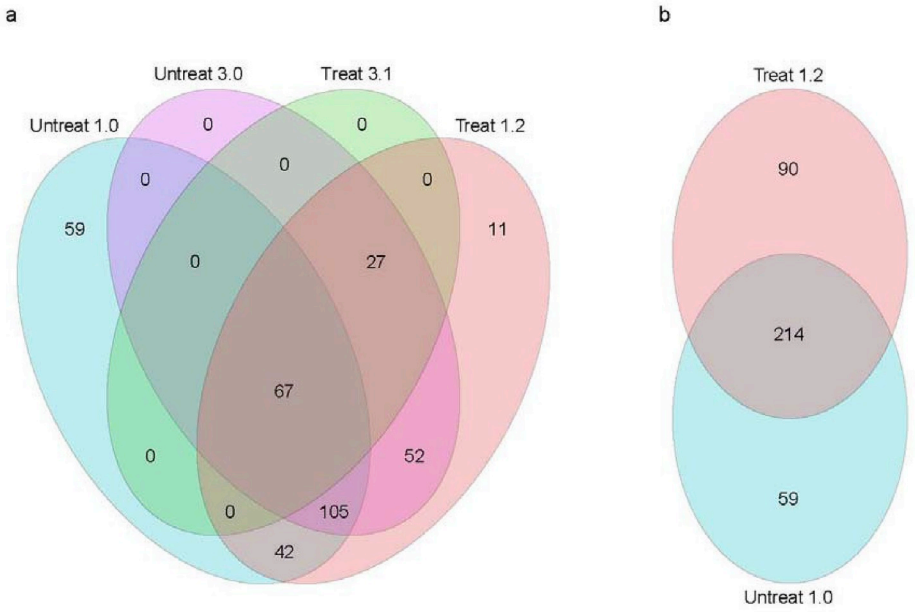


Fig. 6. Venn diagram from OTUs obtained by QIIME 2 performed at Family level showing the abundance of each sample and the intersections between them. A) Venn diagram at Family level regarding all treated and non-treated samples shows the abundance of each sample and the intersections between them. B) Venn diagram at Family level regarding only non-treated sample 1.0 (BRAZIL2) and H_2 treated sample 1.2 (BRAZIL2_C3c).

representing now more than 95% (Fig. 5). This can be also observed by the number of sequences obtained from the starting and treated soil (94 and 251, respectively, Fig. 6a), which represents a loss of 64% in the diversity of bacteria and archaea. The reason for this drastic change in bacterial community structure is likely the treatment temperature, since similar H_2 treatment performed at ambient temperature on the 1.2 sample had a much weaker effect. This assumption is corroborated by the strong capacity of endospore forming *Firmicutes* to withstand extreme conditions owing to the formation of wet-heat-resistant spores (Filippidou et al., 2016). Compared to the average abundance and composition of dominant soil bacterial phylotypes across the globe (Delgado-Baquerizo et al., 2018), the São Francisco soil samples are characterized by a larger proportion of *Chloroflexi* and lower proportion of *Proteobacteria* and *Planctomycetes*. It must be noted that *Chloroflexi* belongs to *Actinobacteria* (Constant et al., 2008, 2010, 2011; Meredith et al., 2014; Greening et al., 2014), and *Acidobacteria* (Greening et al., 2015; Myers and King, 2016) to the three phyla which have been recognized to scavenge atmospheric H_2.

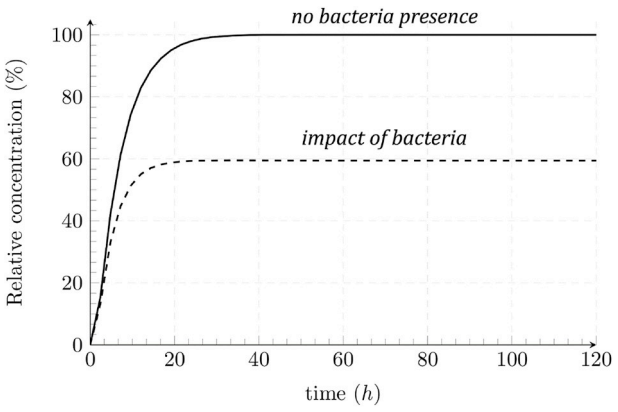


Fig. 7. Effect of bacterial uptake on hydrogen gas concentration measured at the surface as simulated using COMSOL. An infinite source of constant [$H_{2,g}$] is located at the base of a 1-m column. Concentrations are expressed as percent of source concentration. Water saturation is set to 30% and porosity to 0.3. Corresponding diffusive flux in the column is ca. 10^{-9} m^3 [H_2].m^{-2}.s^{-1}.

The effect of H_2 exposure can be visualized on a Venn diagram constructed at family level (Fig. 6) in Rstudio (Version 1.1.456–2009–2018). The intersections (Supplementary Tables A and B) show that all samples together share 67 families where the main phyla present are *Acidobacteria* and *Actinobacteria*. The non-treated sample 1.0 can be directly compared to H_2-treated sample 1.2 since the only variable is the presence or absence of H_2. The 59 unique families present in 1.0 are mainly from the *Proteobacteria* and *Verrucomicrobia* phyla, while the 90 families present only in 1.2 are from the *Actinobacteria*, *Acidobacteria*, *Chloroflexi*, *Firmicutes* and *Proteobacteria* phyla. The intersection between untreated samples 1.0 and 1.2 is mainly dominated by organisms from the *Chloroflexi*, *Actinobacteria*, *Proteobacteria*, *Firmicutes* and *Acidobacteria* phyla.

Compared to samples 1.0, 2.0 and 3.0, sample 4.0 comes from a different locality, differs in its mineralogy (Table 1), and has been stored for a much longer time (Table 2). It is therefore not surprising that sample 4.0 has a distinct bacterial profile. Samples 4.1 and 4.2 could not be amplified with RISA bacterial primers owing to the low amount and integrity of DNA that could be extracted from these samples, which required an incubation time of four weeks before H_2 started to be consumed. Sample 4.1 could also not be amplified with RISA archaeal primers. The long storage time of 15 years might account for the poor bacterial profile with H_2-consumers occurring in the form of spores since H_2-consumption is only triggered after a latency time of several weeks. Similar latency time with respect to H_2 uptake by soil samples has already been reported by McLearn and Dong (2002). Sporulation is the purest form of bacterial dormancy where, upon exposure to favorable conditions, a fraction of spores germinate and initiate rapid growth to reestablish population-promoting long-term survival (Rittershaus et al., 2013). However, although there is an exit from dormancy, the wide range of possible conditions makes such an event challenging (Dworkin and Shah, 2010). Indeed Mukamolova et al. (1998) showed that successful exit from dormancy depends on initial cell concentration and specific laboratory conditions that may actually be different for each microorganism.

3.3. Numerical model of hydrogen diffusive transport across a soil column

In order to comprehend the efficiency of bacteria in removing H_2

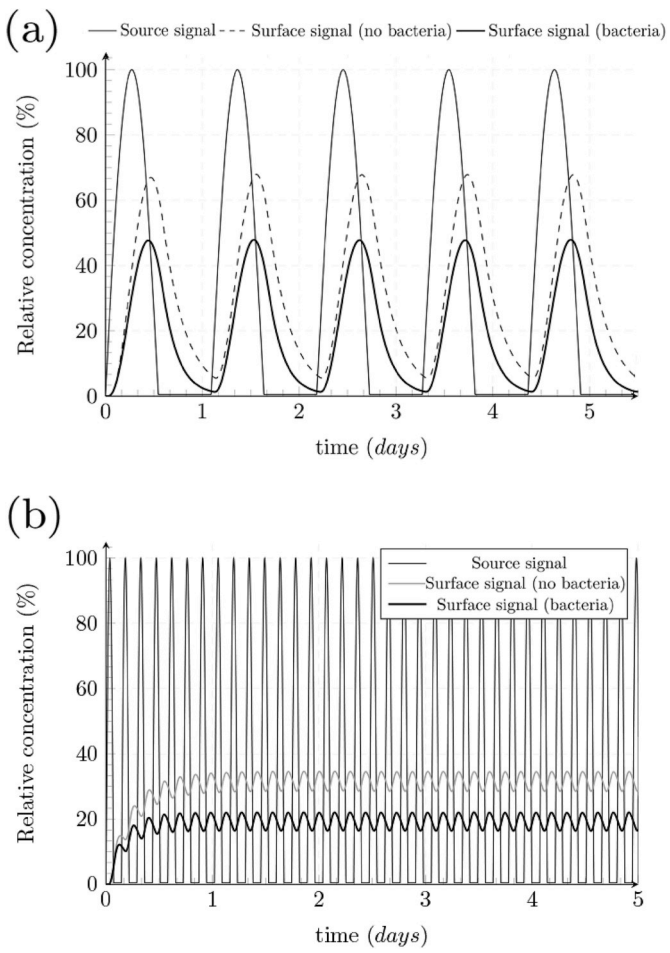


Fig. 8. COMSOL numerical results as for Fig. 7 in the case of sinusoidal pulsing [H_2,g] source at 1-m depth: (a) single [$H_{2,g}$] maximum a day; (b) four [$H_{2,g}$] maximum a day. The bottom source signal is marked as thin black line. Bold black line represents the resulting concentration (bacteria & transport) at the surface. Water saturation is set to 30% and porosity is 0.3.

from the gas phase of the soil porosity, we first calculated, based on the experimental up-take data obtained here, the time required to exhaust an *in-situ* concentration spike of 150 ppm of H_2 of hypothetical origin, assuming a closed and homogeneous system (i.e., no diffusion). It turned out that only 2–9 min are required to return the H_2 concentration to nil. This time is much shorter than the time of 4 h taken by the São Francisco soil to recover background concentration after a concentration pulse (Fig. 4 in Prinzhofer et al., 2019). Therefore a H_2 production flux must operate at São Francisco that counter-balances the effect of bacterial activity in order to maintain H_2 concentrations below background level over several hours (pulsing period). The effect of a H_2 flux on the measured concentration was explored through the numerical modelling of H_2 transfer along an idealized soil column for two cases: a deep source (*Case 1*) and an *in-situ* production in the uppermost 20-cm layer of the 1-D column (*Case 2*).

3.3.1. CASE 1: upward diffusive flow from a deep source

The result in the case of constant hydrogen concentration at the inlet of a flow line (at the depth of 1 m) is presented in Fig. 7. Concentration difference between the top and bottom of the column induces a H_2 diffusing flux through the soil porosity towards the surface. Diffusive spreading is observed with and without H_2-oxidizing bacterial activity. The time required to reach a steady diffusive state is slightly more than 30 h for the considered 1-m column for a pore saturation of 0.3. A sensitivity test showed that a steady state can be reached within a week or more if saturation is increased to 0.7 or if the H_2 source is located at a 3-m depth (Fig. S1).

The impact of H_2-consuming bacteria was considered by introducing a Michaelis-Menten kinetics law, the parameters of which were established on the basis of the experimental results obtained here (Table 3). The overall effect of bacterial activity was found to be remarkable. Indeed, H_2 gas that reaches the surface has a concentration which drops by 40% compared to the infinite bottom source when steady state is reached, and when bacterial H_2 consumption is considered. This bacterial activity tends to be one of the major mechanisms that govern dihydrogen mobility in the subsurface. A primary consequence is that the H_2 concentration at the source can be greatly underestimated if based on the surface or near-surface concentration measurements, depending on the depth of the source and the amount of H_2-consuming bacteria along the diffusion column. It should be noted that adding an advection term and a pressure gradient in the mass transport equation (Eq. (4)) tends to increase the concentration of hydrogen delivered to the surface. Nevertheless, advection does not appear to be the main transport mechanism since the field observations suggest a very low velocity of seeping gas.

In the H_2-emitting structure where the investigated Brazilian soils were sampled, Prinzhofer et al. (2019) detected periodic dihydrogen pulses. This observation led us, in a second approach of *Case 1*, to consider a periodic pulsing H_2 concentration at the bottom of the column instead of a constant concentration. Two different pulse frequencies, 1/24 h^{-1} and 1/6 h^{-1}, at 1 m depth were investigated (Fig. 8a and b, respectively). In Fig. 8, the H_2 (column) surface concentration is displayed assuming diffusive transport with and without bacterial H_2 uptake, respectively. Two main features can be observed in Fig. 8a. First, as a result of diffusion transport, the concentration signal at the surface has a full width at half maximum (FWHM) that is 12% larger compared to the source concentration spike, and a lower amplitude. The amplitude decrease is even more pronounced in the case of H_2 consumption through bacterial activity. Furthermore, the concentration maximum at the surface is shifted by about 4 h compared to the source signal at 1 m. The $\frac{1}{24}$ h^{-1} frequency at the source is characterized by near-zero H_2-concentration episodes at the surface, especially when bacterial activity is involved (Fig. 8a). Increasing the concentration-wave frequency at the source increases the minimum H_2 concentration level at the surface which tends to nearly steady emission of H_2 for $\frac{1}{6}$ h^{-1} (Fig. 8b).

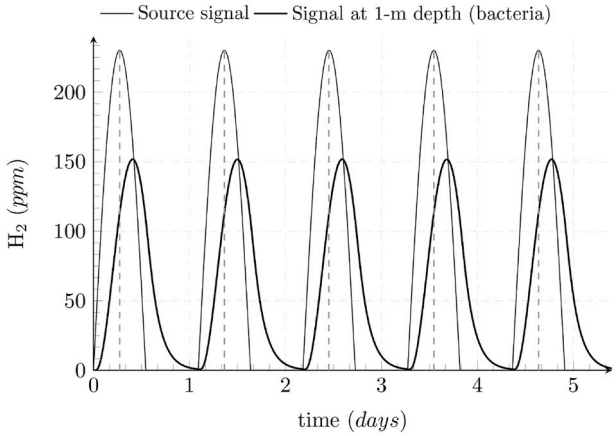


Fig. 9. COMSOL simulated concentration (ppm) of biogenic H_2 produced in the uppermost 20-cm thick layer of the column after it reaches 1-m depth. Thin black line represents the source concentration while the thick line gives the resulting concentration (bacteria & transport) at 1-m depth. Maximum hydrogen production occurs at midday (dashed line). Water saturation is set to 30% and porosity is 0.3.

3.3.2. CASE 2: in-situ H_2 production

A remarkable result obtained by Prinzhofer et al. (2019) on the São Francisco H_2 - emitting structure is that H_2 concentration in soil porosity at 80 cm below the surface correlates well with daily temperature variations. This correlation may suggest a possible link with biological activity, *i.e.* competition between H_2 consumers and producers, the resulting mass balance of which may be temperature dependent. Soil saturation itself can be subjected to daily variations according to evaporation, a process that cannot be ignored at tropical latitudes. When soils dry up, H_2 diffusion out of the soil is expected to be enhanced. Nevertheless, the effect of evaporation appears to be minor in terms of transport via 1-m or even thicker layers of soil, since only the first few centimeters of formation are affected by this process (see below).

In order to achieve an *in-situ* biological H_2 production that correlates with sun exposure and, thus, surface temperature, biogenic gas formation must take place in the first few centimeters of soil that are affected by daily temperature variations. A model, *Case 2*, was simulated assuming a layer of biogenic H_2 production of 20 cm, where calculated temperature variations exceed 1–2 °C. The upper surface of this 20 cm zone is open to the atmosphere. For modelling purposes, producers were homogeneously spread with the consumers in this 20 cm layer, while the other 80 cm of column were filled with H_2 consumers only. The simulated concentrations at 1-m depth are displayed in Fig. 9. Similarly to the previous *Case 1*, there is a delay in the concentration peak and a decrease in the amplitude of the H_2 concentration wave after its production, transport and partial consumption by bacteria. The attenuation of the source maximum [$H_{2,g}$] falls in the 65–67% range at a 1-m depth where the sensor is located.

The maximum concentration value (150 ppm at midday, FWHM = 7 h) measured by Sensor 6 (Fig. 2 *in* Prinzhofer et al., 2019) was inverted in order to infer the concentration amplitude at the source layer (Fig. 9). A production that maintains around 230 ppm at peak is derived assuming a source pulse function with an FWHM of 10 h. The delay in concentration peak arrival may range from 2 to 3.5 h and is highly dependent on the choice of the thickness of H_2-producing layer, porosity, and especially on water saturation in accordance with Equation (3). The numerical analyses show that lowering the saturation of water to 10% from an initial 30% value, which is acceptable due to the overall dryness of the area (Prinzhofer et al., 2019), decreases the characteristic time of peak arrival to less than 2 h from the initial 3.5 h. An evaporation effect can also been introduced into the uppermost 20-cm layer, which enhances H_2 loss towards the atmosphere. Overall, evaporation leads to decrease the maximum [$H_{2,g}$] measured at 1-m depth by only 2% from 67 to 65%.

We calculated that at the maximum daily bacterial production, 96.5% of the hydrogen formed is lost to the atmosphere. On the other hand, only 2.5% of hydrogen would finally arrive to the sensor, and 1% will be consumed by bacteria in the column. Due to such a high flux towards the atmosphere, and in order to maintain 230 ppm at the source layer (Fig. 9), [$H_{2,g}$] production rate in the upper layer has to be around 30 mmol.kg^{-1}day^{-1}. The latter is at least two orders of magnitude higher if compared to the hydrogen consumption rate defined in the current study (Table 3). On the other hand, a H_2 production rate of 30 mmol.kg^{-1}day^{-1} as inferred here, appears to be lower than rates encountered in the case of N_2 fixation associated with legume root nodules. To provide an order of magnitude, the maximum H_2 production flux towards the atmosphere measured above clover fields by Conrad and Seiler (1980) corresponds to a production rate of around 950 mmol H_2.kg^{-1}.day^{-1} if a production zone of 20-cm thickness is considered. Similarly, the production rates estimated by Chen et al. (2015), also recalculated for 20-cm thickness, fall in the range of 15–2000 mmol H_2.kg^{-1}.day^{-1}. The upper bound relates to clover fields whereas the lower bound corresponds to forest sites with no leguminous plants. Therefore, although H_2 production activity in the upper soil layer of the studied H_2-emitting structure has not yet been investigated, production rates inferred from our numerical model are plausible.

3.4. Origin of the H2

The possible biogenic origin of emitted H_2 cannot be ruled out at this point even though the only well-known natural example of strong biogenic H_2 production is associated with nitrogenase in the vicinity of symbiotic root nodules. This symbiotic nitrogenase context hardly applies to the H_2-emitting Brazilian structure studied by Prinzhofer et al. (2019), since it is characterized by a very low density of vegetation. However, detailed analysis of H_2 isotopic signatures of production and uptake of H_2 by soil tends to show that forest sites or bare soils can also produce H_2 even in the absence of leguminous plants (Chen et al., 2015).

Nevertheless, the data recorded by Sensor 9 (Prinzhofer et al., 2019) show no correlation with the solar radiation and indicate concentrations as high as 1000–1200 ppm. The microbial community of the soil sample collected in the vicinity of Sensor 9 does not exhibit significant differences to that collected near Sensor 6, which recorded daily [$H_{2,g}$] variation. The [$H_{2,g}$] signal might therefore rather be a result of superposition of two independent sources, one of deep origin (*Case 1*) and another (*Case 2*) of surface origin, which is influenced by daily temperature variations.

4. Conclusions

We show that H_2-consuming microbial communities in soils act as a major sink for H_2 in the concentration range published for H_2-emitting structures (Larin et al., 2015; Zgonnik et al., 2015; Prinzhofer et al., 2018). For the sandy kaolinite-rich soil collected in the first 15–40 cm of the São Francisco emitting structure, an up-take rate of ca. 0.05 μmol kg^{-1}.d^{-1} was observed in H_2-incubation experiments, which was further investigated in a 1-D diffusion-reaction model. The assumption of a homogeneous distribution of the bacterial up-take activity over the first meter of soil may lead to an overestimate of the overall bacterial up-take derived from the model. On the other hand, several studies point towards the presence of H_2-utilizing bacteria at even deeper levels (Pedersen, 2000; Chapelle et al., 2002; Bagnoud et al., 2016). Thus, the H_2 up-take rate derived here for shallow samples may well be maintained at 1-m depth and beyond. The impact of bacterial H_2 utilization is expected to be even more pronounced for other soil types since H_2 consumption rates by soil bacteria found in the literature can exceed by at least 100 times the rates observed in the present study (Table 3). Situations where dihydrogen produced at depth is completely mediated by bacteria on its way to the surface are thus perfectly conceivable.

The main phyla found in both H_2-treated and non-treated soils are *Firmicutes*, *Chloroflexi*, *Proteobacteria*, *Actinobacteria* and *Acidobacteria*. The composition of these phyla was found to evolve after H_2 treatment, i.e. at the laboratory timescale. It is therefore expected that a H_2-seepage zone will develop a specific bacterial community composition in the percolated soil (*e.g.*, abundant *Chloroflexi*).

Finally, the present study does not provide a definite answer about the origin of the H_2 that is emitted by the circular Brazilian depression instrumented by Prinzhofer et al. (2019). However, we have produced a first modelling tool to interpret forthcoming H_2-concentration data that will be collected in similar structures encountered worldwide. Further deeper drilling for H_2 flux and concentration measurements may provide pivotal data to constrain the H_2 dynamics discussed here. Constraints on the 3D distribution of microbiological communities within the emitting structure, and their interaction with H_2, are obviously of primary importance to characterize the H_2 source.

Declaration of competing interest

The authors declare that they have no known competing financial interests or personal relationships that could have appeared to influence the work reported in this paper.

Acknowledgments

ENGIE funded this work as well as the monitoring of the structure in Brazil. Additional funding from CNRS/INSU through the TelluS Program is also acknowledged. IRD financed FB stay at the Cell Biology Dept. of Brasilia University. RK would like to thank CNPq, CAPES and FAPDF for financial support. We also thank S. Guédron for providing us with the Guiana soils, N. Finding for acquisition and interpretation of the XRD patterns, A. Prinzhofer for fruitful discussions and his inexhaustible enthusiasm about natural H_2 research, J. B. Françolin for his kind help with Brazilian soils sampling and handling. Chemical analyses of the soil sample chemistry was carried out at the *Service d'Analyse des Roches et des Minéraux* (SARM, CNRS-CRPG, Nancy, France). The anonymous reviewer is acknowledged for a constructive and detailed review of the manuscript.

Appendix A. Supplementary data

Supplementary data to this article can be found online at https://doi.org/10.1016/j.apgeochem.2019.104474.

References

Bagnoud, A., Leupin, O., Schwyn, B., Bernier-Latmani, R., 2016. Rates of microbial hydrogen oxidation and sulfate reduction in Opalinus Clay rock. Appl. Geochem. 72, 42–50.

Briere, D., Jerzykiewicz, T., 2016. On generating a geological model for hydrogen gas in the southern Taoudeni Megabasin (Bourakebougou area, Mali). In: International Conference and Exhibition, Barcelona, Spain, 3-6 April 2016, p. 342.

Chapelle, F.H., O'Neill, K., Bradley, P.M., Methé, B.A., Ciufo, S.A., Knobel, L.L., Lovley, D.R., 2002. A hydrogen-based subsurface microbial community dominated by methanogens. Nature 415, 312–315.

Chen, Q., Popa, M.E., Batenburg, A.M., Röckmann, T., 2015. Isotopic signatures of production and uptake of H_2 by soil. Atmos. Chem. Phys. 15 (22), 13003–13021.

Conrad, R., Seiler, W., 1979. Field measurements of hydrogen evolution by nitrogen-fixing legumes. Soil Biol. Biochem. 11, 689–690.

Conrad, R., Seiler, W., 1980. Contribution of hydrogen production by biological nitrogen fixation to the global hydrogen budget. J. Geophys. Res. 85, 5493–5498.

Conrad, R., Seiler, W., 1981. Decomposition of atmospheric hydrogen by soil microorganisms and soil enzymes. Soil Biol. Biochem. 13 (1), 43–49. https://doi.org/10.1016/0038-0717(81)90101-2.

Conrad, R., Seiler, W., 1985. Influence of temperature, moisture, and organic carbon on the flux of H_2 and CO between soil and atmosphere: field studies in subtropical regions. J. Geophys. Res.: Atmos. 90 (D3), 5699–5709. https://doi.org/10.1029/JD090iD03p05699.

Constant, P., Poissant, L., Villemur, R., 2008. Isolation of Streptomyces sp. PCB7, the first microorganism demonstrating high-affinity uptake of tropospheric H_2. ISME J. 2, 1066–1076. https://doi.org/10.1038/ismej.2008.59.

Constant, P., Chowdhury, S.P., Pratscher, J., Conrad, R., 2010. Streptomycetes contributing to atmospheric molecular hydrogen soil uptake are widespread and encode a putative high-affinity [NiFe]-hydrogenase. Environ. Microbiol. 12 (3), 821–829. https://doi.org/10.1111/j.1462-2920.2009.02130.x.

Constant, P., Chowdhury, S.P., Hesse, L., Pratscher, J., Conrad, R., 2011. Genome data mining and soil survey for the Novel Group 5 [NiFe]-Hydrogenase to explore the diversity and ecological importance of presumptive high-affinity H_2-oxidizing bacteria. Appl. Environ. Microbiol. 77 (17), 6027. https://doi.org/10.1128/AEM.00673-11.

Crozier, T.E., Yamamoto, S., 1974. Solubility of hydrogen in water, sea water, and sodium chloride solutions. J. Chem. Eng. Data 19 (3), 242–244. https://doi.org/10.1021/je60062a007.

Delgado-Baquerizo, M., Oliverio, A.M., Brewer, T.E., Benavent-González, A., Eldridge, D. J., Bardgett, R.D., Maestre, F.T., Singh, B.K., Fierer, N., 2018. A global atlas of the dominant bacteria found in soil. Science 359 (6373), 320–325. https://doi.org/10.1126/science.aap9516.

Dong, Z., Layzell, D.B., 2001. H_2 oxidation, O_2 uptake and CO_2 fixation in hydrogen treated soils. Plant Soil 229 (1), 1–12. https://doi.org/10.1023/A:1004810017490.

Dong, Z., Wu, L., Kettlewell, B., Caldwell, C.D., Layzell, D.B., 2003. Hydrogen fertilization of soils - is this a benefit of legumes in rotation? Plant Cell Environ. 26 (11), 1875–1879. https://doi.org/10.1046/j.1365-3040.2003.01103.x.

Dworkin, J., Shah, I.M., 2010. Exit from dormancy in microbial organisms. Nat. Rev. Microbiol. 8 (12), 890–896. https://doi.org/10.1038/nrmicro2453.

Ehhalt, D.H., Schmidt, U., Heidt, L.E., 1977. Vertical profiles of molecular hydrogen in the troposphere and stratosphere. J. Geophys. Res. 82 (37), 5907–5911. https://doi.org/10.1029/JC082i037p05907.

Ferrell, R.T., Himmelblau, D.M., 1967. Diffusion coefficients of hydrogen and helium in water. AIChE J. 13 (4), 702–708. https://doi.org/10.1002/aic.690130421.

Filippidou, S., Wunderlin, T., Junier, T., Jeanneret, N., Dorador, C., Molina, V., Johnson, D.R., Junier, P., 2016. A combination of extreme environmental conditions favor the prevalence of endospore-forming Firmicutes. Front. Microbiol. 7 https://doi.org/10.3389/fmicb.2016.01707.

Garcia-Martinez, J., Rodriguez-Valera, F., 2000. Microdiversity of uncultured marine prokaryotes: the SAR11 cluster and the marine Archaea of Group I. Mol. Ecol. 9 (7), 935–948. https://doi.org/10.1046/j.1365-294x.2000.00953.x.

Gödde, M., Meuser, K., Conrad, R., 2000. Hydrogen consumption and carbon monoxide production in soils with different properties. Biol. Fertil. Soils 32 (2), 129–134. https://doi.org/10.1007/s003740000226.

Greening, C., Berney, M., Hards, K., Cook, G.M., Conrad, R., 2014. A soil actinobacterium scavenges atmospheric H2 using two membrane-associated, oxygen-dependent [NiFe] hydrogenases. Proc. Natl. Acad. Sci. 111 (11), 4257–4261. https://doi.org/10.1073/pnas.1320586111.

Greening, C., Carere, C.R., Rushton-Green, R., Harold, L.K., Hards, K., Taylor, M.C., Morales, S.E., Stott, M.B., Cook, G.M., 2015. Persistence of the dominant soil phylum *Acidobacteria* by trace gas scavenging. Proc. Natl. Acad. Sci. 112 (33), 10497. https://doi.org/10.1073/pnas.1508385112.

Guedron, S., Grangeon, S., Lanson, B., Grimaldi, M., 2009. Mercury speciation in a tropical soil association; Consequence of gold mining on Hg distribution in French Guiana. Geoderma 153 (3), 331–346. https://doi.org/10.1016/j.geoderma.2009.08.017.

Häring, V., Conrad, R., 1994. Demonstration of two different H_2-oxidizing activities in soil using an H_2 consumption and a tritium exchange assay. Biol. Fertil. Soils 17 (2), 125–128. https://doi.org/10.1007/BF00337744.

Islam, Z.F., Cordero, P.R.F., Feng, J., Chen, Y.J., Bay, S.K., Jirapanjawat, T., Gleadow, R. M., Carere, C.R., Stott, M.B., Chiri, E., Greening, C., 2019. Two Chloroflexi classes independently evolved the ability to persist on atmospheric hydrogen and carbon monoxide. ISME J. 13 (7), 1801–1813. https://doi.org/10.1038/s41396-019-0393-0.

Janecky, D.R., Seyfried, W.E., 1986. Hydrothermal serpentinization of peridotite within the oceanic crust: experimental investigations of mineralogy and major element chemistry. Geochem. Cosmochim. Acta 50 (7), 1357–1378. https://doi.org/10.1016/0016-7037(86)90311-X.

Khdhiri, M., Hesse, L., Popa, M.E., Quiza, L., Lalonde, I., Meredith, L.K., Rockman, T., Constant, P., 2015. Soil carbon content and relative abundance of high affinity H_2-oxidizing bacteria predict atmospheric H_2 soil uptake activity better than soil microbial community composition. Soil Biol. Biochem. 85, 1–9. https://doi.org/10.1016/j.soilbio.2015.02.030.

La Favre, J.S., Focht, D.D., 1983. Conservation in soil of H_2 liberated from N_2 fixation by hup- nodules. Appl. Environ. Microbiol. 46 (2), 304–311.

Larin, N.V., Larin, V.N., Gorbatikov, A.V., 2010. Ring structures due to deep hydrogen flows. Degazaciya Zemli: geotektonika, geodinamika, geoflyuidy; neft' i gaz; uglevodorody i zhizn': mater. Vseros. konf. (Earth degassing: geotectonics, geodynamics, geofluids; oil and gas; hydrocarbons and life. In: Proc. All-Russ. conf. Moscow. GEOS, pp. 284–288 (In Russ.).

Larin, N., Zgonnik, V., Rodina, S., Deville, E., Prinzhofer, A., Larin, V.N., 2015. Natural molecular hydrogen seepage associated with surficial, rounded depressions on the European craton in Russia. Nat. Resour. Res. 24 (3), 369–383. https://doi.org/10.1007/s11053-014-9257-5.

Lopez-Lazaro, C., Bachaud, P., Moretti, I., Ferrando, N., 2019. Predicting the phase behavior of hydrogen in NaCl brines by molecular simulation for geological applications. BSGF - Earth Sci. Bull 190 (7). https://doi.org/10.1051/bsgf/2019008.

McLearn, N., Dong, Z., 2002. Microbial nature of the hydrogen-oxidizing agent in hydrogen-treated soil. Biol. Fertil. Soils 35 (6), 465–469. https://doi.org/10.1007/s00374-002-0495-z.

Meredith, L.K., Rao, D., Bosak, T., Klepac-Ceraj, V., Tada, K.R., Hansel, C.M., Ono, S., Prinn, R.G., 2014. Consumption of atmospheric hydrogen during the life cycle of soil-dwelling actinobacteria: uptake of H_2 during the life cycle of soil actinobacteria. Environ. Microbiol. Rep. 6 (3), 226–238. https://doi.org/10.1111/1758-2229.12116.

Millington, R.J., Quirk, J.P., 1961. Permeability of porous solids. Trans. Faraday Soc. 57, 1200–1207.

Mukamolova, G.V., Yanopolskaya, N.D., Kell, D.B., Kaprelyants, A.S., 1998. On resuscitation from the dormant state of Micrococcus luteus. Antonie Leeuwenhoek 73 (3), 237–243. https://doi.org/10.1023/A:1000881918216.

Myers, M.R., King, G.M., 2016. Isolation and characterization of Acidobacterium ailaaui sp. nov., a novel member of Acidobacteria subdivision 1, from a geothermally heated Hawaiian microbial mat. Int. J. Syst. Evol. Microbiol. 66 (12), 5328–5335. https://doi.org/10.1099/ijsem.0.001516.

Nandi, R., Sengupta, S., 1998. Microbial production of hydrogen: an overview. Crit. Rev. Microbiol. 24 (1), 61–84. https://doi.org/10.1080/10408419891294181.

Nieber, J.L., Sidle, R.C., Wilson, G.V., Fox, G.A., 2013. Connectivity of preferential pathways for flow and transport in soils. AGU Fall Meet. Abstr. 11, H11I–H1258.

Nivin, V.A., Pukha, V.V., Lovchikov, A.V., Rakhimov, R.G., 2016. Changes in the molecular hydrogen concentration in an underground mine (Lovozero rare-metal deposit, Kola Peninsula). Dokl. Earth Sci. 471 (2), 1261–1264. https://doi.org/10.1134/S1028334X16120060.

Normand, P., Ponsonnet, C., Nesme, X., Neyra, M., Simonet, P., 1996. ITS analysis of prokaryotes. In: Akkermans, D.L., van Elsas, J.D., De Bruijn, E.L. (Eds.), Molecular Microbial Ecology Manual. Kluwer Academic Publishers, Amsterdam, pp. 1–12.

Pedersen, K., 2000. Exploration of deep intraterrestrial microbial life: current perspectives. FEMS Microbiol. Lett. 185, 9–16.

Perner, M., Petersen, J.M., Zielinski, F., Gennerich, H.H., Seifert, R., 2010. Geochemical constraints on the diversity and activity of H 2-oxidizing microorganisms in diffuse hydrothermal fluids from a basalt- and an ultramafic-hosted vent. FEMS (Fed. Eur. Microbiol. Soc.) Microbiol. Ecol. 74 (1), 55–71. https://doi.org/10.1111/j.1574-6941.2010.00940.x.

Piché-Choquette, S., Tremblay, J., Tringe, S.G., Constant, P., 2016. H_2-saturation of high affinity H_2-oxidizing bacteria alters the ecological niche of soil microorganisms unevenly among taxonomic groups. PeerJ 4, e1782. https://doi.org/10.7717/peerj.1782.

Piché-Choquette, S., Khdhiri, M., Constant, P., 2018. Dose-response relationships between environmentally-relevant H_2 concentrations and the biological sinks of H_2, CH_4 and CO in soil. Soil Biol. Biochem. 123, 190–199. https://doi.org/10.1016/j.soilbio.2018.05.008.

Popelier, F., Liessens, J., Verstraete, W., 1985. Soil H_2-uptake in relation to soil properties and rhizobial H_2-production. Plant Soil 85 (1), 85–96. https://doi.org/10.1007/BF02197803.

Prinzhofer, A., Tahara Cissé, C.S., Diallo, A.B., 2018. Discovery of a large accumulation of natural hydrogen in Bourakebougou (Mali). Int. J. Hydrogen Energy 43 (42), 19315–19326. https://doi.org/10.1016/j.ijhydene.2018.08.193.

Prinzhofer, A., Moretti, I., Françolin, J., Pacheco, C., D'Agostino, A., Werly, J., Rupin, F., 2019. Natural hydrogen continuous emission from sedimentary basins: the example of a Brazilian H_2-emitting structure. Int. J. Hydrogen Energy 44 (12), 5676–5685. https://doi.org/10.1016/j.ijhydene.2019.01.119.

Rittershaus, E.S.C., Baek, S.H., Sassetti, C.M., 2013. The normalcy of dormancy: common themes in microbial quiescence. Cell Host Microbe 13 (6), 643–651. https://doi.org/10.1016/j.chom.2013.05.012.

Savary, V., Pagel, M., 1997. The effects of water radiolysis on local redox conditions in the Oklo, Gabon, natural fission reactors 10 and 16. Geochem. Cosmochim. Acta 61 (21), 4479–4494. https://doi.org/10.1016/S0016-7037(97)00261-5.

Schmidt, U., 1978. The latitudinal and vertical distribution of molecular hydrogen in the troposphere. J. Geophys. Res. 83 (C2), 941. https://doi.org/10.1029/JC083iC02p00941.

Schuler, S., Conrad, R., 1990. Soils contain two different activities for oxidation of hydrogen. FEMS (Fed. Eur. Microbiol. Soc.) Microbiol. Ecol. 6 (1), 77–83. https://doi.org/10.1111/j.1574-6968.1990.tb03927.x.

Sequerra, J., Marmeisse, R., Valla, G., Normand, P., Capellano, A., Moiroud, A., 1997. Taxonomic position and intraspecific variability of the nodule forming Penicillium nodositatum inferred from RFLP analysis of the ribosomal intergenic spacer and Random Amplified Polymorphic DNA. Mycol. Res. 101 (4), 465–472.

Smith-Downey, N.V., Randerson, J.T., Eiler, J.M., 2006. Temperature and moisture dependence of soil H_2 uptake measured in the laboratory. Geophys. Res. Lett. 33 (14) https://doi.org/10.1029/2006GL026749.

Sukhanova, N.I., Trofimov, S.Y., Polyanskaya, L.M., Larin, N.V., Larin, V.N., 2013. Changes in the humus status and the structure of the microbial biomass in hydrogen exhalation places. Eurasian Soil Sci. 46 (2), 135–144. https://doi.org/10.1134/S1064229313020142.

Trevors, J.T., 1985. Hydrogen consumption in soil. Plant Soil 87 (3), 417–422. https://doi.org/10.1007/BF02181908.

Truche, L., Joubert, G., Dargent, M., Martz, P., Cathelineau, M., Rigaudier, T., Quirt, D., 2018. Clay minerals trap hydrogen in the Earth's crust: evidence from the Cigar Lake uranium deposit, Athabasca. Earth Planet. Sci. Lett. 493, 186–197. https://doi.org/10.1016/j.epsl.2018.04.038.

Wakita, H., Nakamura, Y., Kita, I., Fujii, N., Notsu, K., 1980. Hydrogen release: new indicator of fault activity. Science 210 (4466), 188–190. https://doi.org/10.1126/science.210.4466.188.

Yashiro, H., Sudo, K., Yonemura, S., Takigawa, M., 2011. The impact of soil uptake on the global distribution of molecular hydrogen: chemical transport model simulation. Atmos. Chem. Phys. 11, 6701–6719. https://doi.org/10.5194/acp-11-6701-2011.

Yonemura, S., Kawashima, S., Tsuruta, H., 1999. Continuous measurements of CO and H_2 deposition velocities onto an andisol: uptake control by soil moisture. Tellus B Chem. Phys. Meteorol. 51, 688–700. https://doi.org/10.3402/tellusb.v51i3.16465.

Yonemura, S., Kawashima, S., Tsuruta, H., 2000. Carbon monoxide, hydrogen, and methane uptake by soils in a temperate arable field and a forest. J. Geophys. Res. 105, 14347–14362. https://doi.org/10.1029/1999JD901156.

Yonemura, S., Yokozawa, M., Kawashima, S., Tsuruta, H., 2000. Model analysis of the influence of gas diffusivity in soil on CO and H_2 uptake. Tellus B Chem. Phys. Meteorol. 52, 919–933. https://doi.org/10.3402/tellusb.v52i3.17075.

Zgonnik, V., Beaumont, V., Deville, E., Larin, N., Pillot, D., Farrell, K.M., 2015. Evidence for natural molecular hydrogen seepage associated with Carolina bays (surficial, ovoid depressions on the Atlantic Coastal Plain, Province of the USA). Prog. Earth Planet. Sci. 2 (1), 31. https://doi.org/10.1186/s40645-015-0062-5.